VIP Nanostructure Assembly

DOI: 10.1002/ange.201005365

Building Hematite Nanostructures by Oriented Attachment**

*Jun Song Chen, Ting Zhu, Chang Ming Li, and Xiong Wen Lou**

Oriented attachment (OA) is one of the important mechanisms that govern the crystal growth in the nanoscale regime.[1,2] Unlike the classic kinetics of Ostwald ripening, which is widely used to explain the formation of complex nanostructure such as hollow nanomaterials,[3–8] the essence of OA is that small nanocrystals with common crystallographic orientation aggregate and form larger ones.[9] The attachment of these primary nanoparticles are irreversible and occurs in a highly oriented manner, leading to the elimination of the interfaces of the joint crystals[9] and the formation of chemical bonds after the removal of the solvent and/or adsorbed molecules at these interfaces.[10] Thus, the reduction of the surface energy and the increase in entropy serve as the driving force for the OA growth process.[9,10]

To date, the OA mechanism has been clearly observed in a wide range of crystal structures, including PbSe,[11] ZnO and ZnS,[12–15] TiO_2,[10,16–18] and copper- or iron-based materials.[19–23] The primary building blocks in these works are generally nanoparticles of relatively small size and weight,[9] and there have been rare examples showing the OA of primary nanocrystals of larger size, for example more than than 50 nm. Moreover, these primary nanoparticles can achieve crystallographic accordance in mainly one preferred direction. This preference usually constrains the OA to be unidirectional, and thus mainly one-dimensional (1D) structures are formed in most of the cases. There is no work demonstrating the synthesis of two-dimensional (2D),[1] or even three-dimensional (3D) quasi single crystals by OA. As reported previously, 2D or 3D hierarchical structures assembled from large functional subunits have intriguing properties for applications in different fields.[24,25] It is worth mentioning that the actual active components in many devices are indeed the assemblies of individual particles instead of the subunits which perform different useful actions, such as charge transduction in solar cells or light emission in LEDs.[26] It is thus desirable to overcome the above-mentioned two limitations of OA and thus create opportunities of generating novel materials with potentials for different applications.[26]

Herein, we present the formation of 1D and 2D assemblies of hematite (α-Fe_2O_3) nanoparticles by OA. A simple hydrothermal route is employed by directly aging the $FeCl_3$ aqueous solution at a relatively low temperature of 105 °C, and the as-prepared α-Fe_2O_3 nanoparticles subunits constituting the assemblies are of about 100 nm in size, which is significantly larger than those reported previously. 1D chain-like structures (designated as sample I) are first formed by OA of these large nanoparticles during the early stage of the reaction. With prolonged reaction, more building blocks were attached, which led to not only the extension in the longitudinal axis, but also expansion in both lateral sides. This expansion gives rise to the formation of large 2D layers of α-Fe_2O_3 nanoparticles (designated as sample II). We further demonstrate that these 2D single-layer structures can stack along the [001] direction by magnetic dipole–dipole interactions to form a 3D superstructure (designated as sample III) over long distances. Moreover, based on shape selectivity, we show that 3D α-Fe_2O_3 quasi cubes can be produced by OA of α-Fe_2O_3 nanorods.

Figure 1 A shows the transmission electron microscopy (TEM) image of sample I after the hydrothermal treatment of 12 h; a large portion of free-standing α-Fe_2O_3 nanoparticles with an average size of 100 nm can be clearly observed. At the same time, a considerable amount of chain-like assemblies consisting of various numbers of building blocks co-exist with

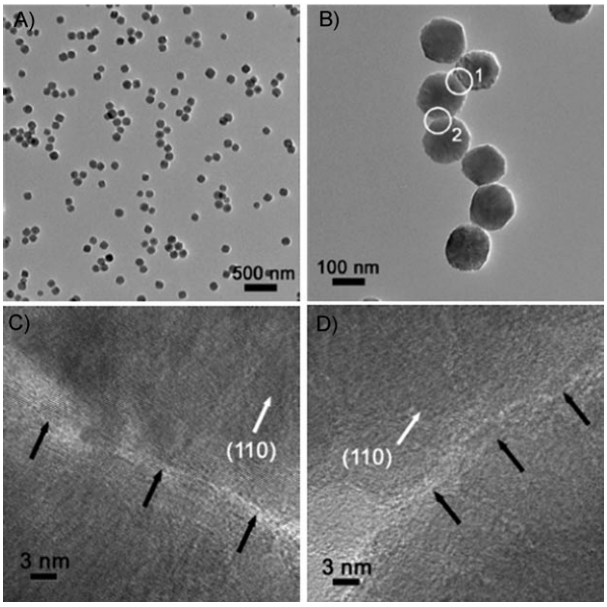

Figure 1. A,B) Transmission electron microscopy (TEM) images of sample I. C,D) High-resolution TEM (HRTEM) images of the regions 1 (C) and 2 (D) marked by white circles in (B). The black arrows indicate the particle boundaries.

[*] J. S. Chen, T. Zhu, Prof. C. M. Li, Prof. X. W. Lou
School of Chemical and Biomedical Engineering
Nanyang Technological University
70 Nanyang Drive, Singapore 637457 (Singapore)
E-mail: xwlou@ntu.edu.sg

[**] We thank all the referees for the encouraging comments, Prof. Hua Chun Zeng (NUS, Singapore) for proof-reading the manuscript, and Prof. Chi Bun Ching for generous support in experimental facilities. X.W.L. is grateful to the Ministry of Education (Singapore) for financial support through the AcRF Tier-1 funding (RG 63/08, M52120096).

Supporting information for this article is available on the WWW under http://dx.doi.org/10.1002/anie.201005365.

the individual particles, and these 1D aggregates may be regarded as the secondary structure. One of these 1D structures composed of 7 α-Fe_2O_3 nanocrystals is displayed under higher magnification (Figure 1B), which assumes an epitaxial assembly of the subunits along its longitudinal axis.[21] These primary nanocrystals are almost isotropic or quasi-hexagonal from the direction of observation. High-resolution (HR) TEM images are taken at the boundaries between the second and the third (Figure 1C) and the third and the fourth building blocks (Figure 1D). Clearly almost identical crystallographic orientations can be found on either side of the particle border in both regions. This observation shows that OA is the underlying mechanism responsible for the low-dimensional assembly of these large α-Fe_2O_3 nanocrystals.

Figure 2A shows the morphology of sample II after prolonged treatment up to 25 h. A large number of 2D single-layer assemblies of the primary nanocrystals can be identified, and they are referred as the tertiary structure. One

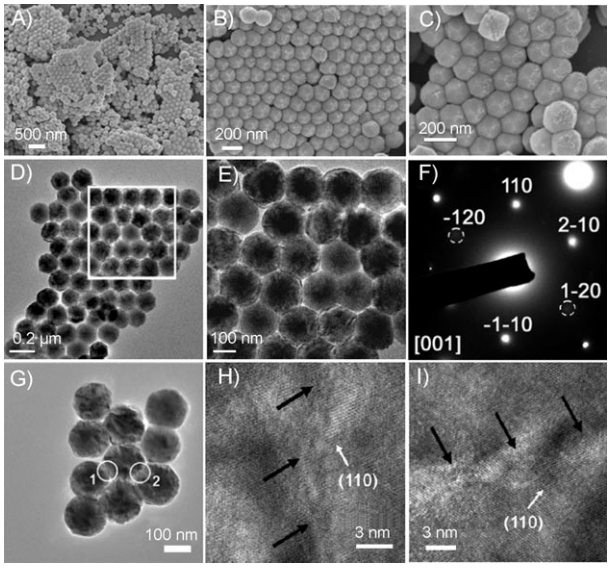

Figure 2. A–C) SEM and D–F) TEM images of sample II. E) A magnified image of the region marked by a white square in (D). F) The selected-area electron diffraction (SAED) pattern of sample II. H,I) HRTEM images of the regions 1 and 2 (marked by white circles) in (G). The black arrows indicate the particle boundaries.

piece of these 2D single-layer structures is illustrated in Figure 2B; it consists of many building blocks arranged in a highly ordered manner, albeit with some obvious misorientations in the center of the assembly. It is suggested that these growth defects can lower the activation barrier, leading to increased rates of subsequent reactions.[1] When viewed under higher magnification (Figure 2C), these subunits seem to adopt a quasi-hexagonal shape, and each one of them is surrounded by six neighboring particles. Such interesting single-layer structure is confirmed under TEM (Figure 2D), and the primary building blocks are indeed isotropic with no pronounced facets (Figure 2E). The selected-area electron diffraction (SAED) pattern (Figure 2F) evidently reveals the single-crystalline nature of these 2D assemblies.[2]

HRTEM was again applied at two different boundary regions from a smaller structure (Figure 2G), and the obtained results (Figure 2H,I) indicate that OA is also the governing mechanism for this 2D assembly because of the crystallographic accordance of the adjacent nanocrystals. From these HRTEM images, two sets of clear lattice fringes with equal interplanar distance at an angle of 60° can be observed, implying that these primary α-Fe_2O_3 nanocrystals are lying on their (001) plane.[27,28] In general, it is more favorable for the oriented aggregation of α-Fe_2O_3 nanocrystals to take place on the (001) facets than on other planes, because the (001) plane of α-Fe_2O_3 has a low surface energy, whose value is calculated to be between 0.75 and 1.65 $J\,m^{-2}$, depending on the environment.[22] However, because that all spins of adjacent Fe layers in α-Fe_2O_3 are parallel in the (001) plane, the horizontal orientation of these dipoles could be energetically preferred owing to a larger mutual connectivity of dipole moments.[29] This effect may explain the observed oriented attachment on (110) facets in present study.

We hypothesize that these 2D assemblies are formed as follows. The pre-assembled 1D chain-like structures serve as nucleation centers, to which the individual nanocrystals attach, most likely through Brownian motion-driven interparticle collisions.[1] Furthermore, in-situ rotations of these primary building blocks within the assembly are also possible,[1] allowing them to find the proper configurations with matching crystallographic orientation across neighboring particles. The abundant water molecules in the present aqueous system may act like a coordinating factor on the iron oxide surface, and the energy required to form such assemblies is relatively low because of the absence of passivating agents.[10] It is worth mentioning that by nature such 2D assemblies by OA are highly stable: they will not break up into individual particles even after 1 h of ultrasonication.

Extending the reaction further to 50 h leads to stacking of the 2D assemblies and formation of more complex quaternary 3D superstructures in sample III (Figure 3A), with a large number of the 2D tertiary structures aligning parallel to each other along the [001] direction. The enlarged view (Figure 3B) illustrates that the stacking is highly organized, and space between adjacent layers can be observed. From this figure, the α-Fe_2O_3 primary building blocks can be viewed as bipyramids with truncated edges and apexes. The structural inhomogeneity of these subunits leads to the topographical mismatching of adjacent 2D layers, preventing them from attaching with one another over a large area. Oriented attachment is thus less likely to occur under such circumstances, and we attribute the formation of these 3D assemblies to the magnetic dipole–dipole interactions between neighboring 2D layers. It has previously been discussed that the dipole moment is rather small in antiferromagnetic α-Fe_2O_3 nanocrystals that are tens of nanometers in size, and thus the dipole–dipole interaction is too weak to give rise to any correlation of these nanoparticles in a particular direction such as [001].[30,31] In present study, however, numerous circa 100 nm α-Fe_2O_3 nanocrystals assemble by oriented attach-

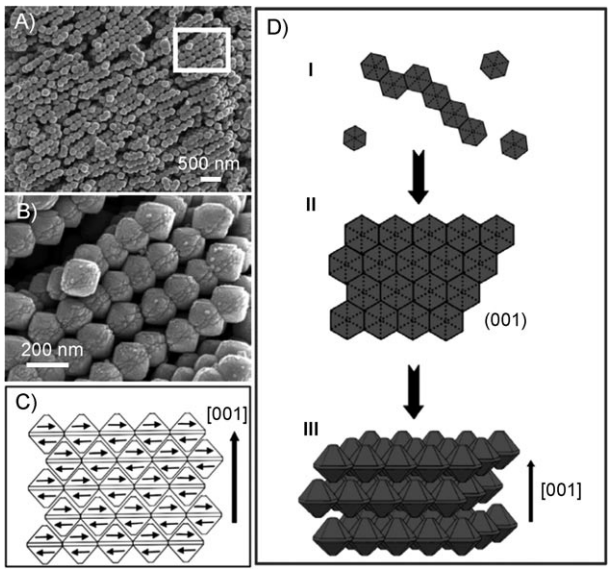

Figure 3. A,B) SEM images showing the side view of sample III. B) Magnified image of the region marked by the white square in (A). C) The antiferromagnetic correlation across the 2D assemblies in sample III. D) Illustration of the formation of the α-Fe_2O_3 structures. Sample I is formed by the oriented attachment of the primary α-Fe_2O_3 nanocrystals. After prolonged reaction, these 1D assemblies evolve into tertiary 2D structures through oriented attachment of nanocrystals (sample II). After 50 h, these 2D assemblies stack together along the [001] direction to form quaternary 3D architecture based on magnetic dipole–dipole interactions (sample III).

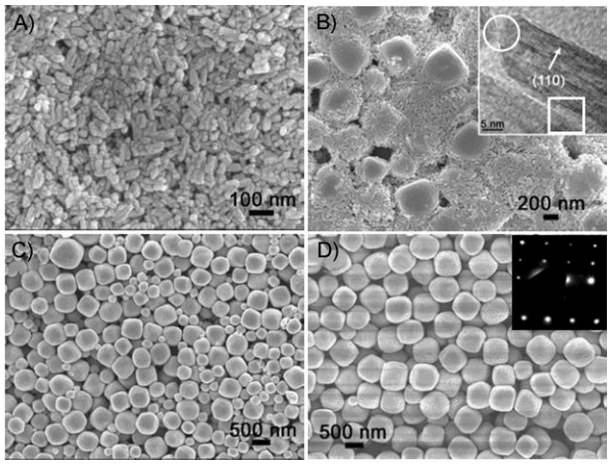

Figure 4. SEM images showing the structural evolution of β-FeOOH nanorods to α-Fe_2O_3 quasi nanocubes for different reaction durations: A) 1 h, B) 3 h, C) 6 h, D) 12 h. Insets in (B) and (D) are a HRTEM image and a SAED pattern of the corresponding sample, respectively.

ment to form a large single-crystalline 2D structure perpendicular to the [001] direction. These orderly arranged primary subunits will probably contribute to a greatly enhanced total dipole moment of the tertiary 2D assemblies, which is strong enough to bring these 2D single-layer structures to close proximity and align along their [001] axis (Figure 3C), thus leading to the quaternary 3D superstructures. The structural evolution from primary building blocks to quaternary 3D superstructure is illustrated in Figure 3D. The chemical compositions of the three samples are confirmed by X-ray diffraction (XRD), and the results (Supporting Information, Figure S1) show phase-pure rhombohedral iron oxide (α-Fe_2O_3, JCPDS card no.: 33-0664).[32]

From the above discussion, we have suggested that owing to the special bipyramidal structure of the α-Fe_2O_3 nanocrystals, OA is not responsible for the 3D assemblies of the 2D structures. However, by switching the nanocrystals to 1D nanorods, we are able to build 3D nanocubes by the same OA process from initial rod-shaped subunits (Figure 4). Free-standing nanorods that are tens of nanometers in thickness and about 100 nm in length are first formed after hydrothermal treatment of 1 h (Figure 4A). The chemical composition of these nanorods is confirmed by XRD analysis (Supporting Information, Figure S2, pattern I) to be phase-pure β-FeOOH (JCPDS No. 75-1594). When the reaction is prolonged to 3 h, the metastable β-FeOOH has completely transformed into α-Fe_2O_3 under the present hydrothermal treatment (Supporting Information, Figure S2, pattern II).[33] It is clear from the image (Figure 4B) that some much larger particles with varying sizes emerge from these nanorods. They can be probably viewed as the top facets of some cubic structures, which are built from the small nanorods with a specific arrangement. The inset in Figure 4B shows a HRTEM image of the tip of one nanorod constituting the cubic particles. It connects and attaches to the neighboring nanorods in both longitudinal and lateral directions. The similarity in the crystallographic orientation can be clearly identified across adjacent rods at both the end-to-end (indicated by the upper white circle) and the side-by-side joint regions (lower white square), evidently proving that oriented attachment is the underlying mechanism responsible for the formation of the secondary cube-like structures from the small nanorods. Further extending the reaction to 6 h leads to the disappearance of nanorods in the product, which totally consists of large quasi cubes (Figure 4C). These nanocubes are with rounded edges and truncated corners, and their size is also divergent from about 100 nm to more than 500 nm. The smaller nanocubes can no longer be found after 12 h of reaction, and only larger cubes of about 500 nm in size can be observed with relatively uniform size distribution (Figure 4D). The inset in Figure 4D shows the SAED pattern of a single nanocube, revealing its single crystallinity.

Based on the above observations, we hypothesize the formation mechanism of the uniform quasi nanocubes. During the early stage of reaction, freely movable nanorods start to aggregate with one another longitudinally and laterally by OA. This attachment process continues to give rise to a 3D cube-shaped structure. Due to the discrepancies in the morphology of the primary nanorods, the resultant quasi nanocubes are with a relatively broad size distribution. Based on work on direct assembly of secondary structures,[9] we believe that these smaller nanocubes can aggregate together by OA to form large single-crystalline quasi-cubic structures upon prolonged reaction. Ostwald ripening should also be partly responsible for the formation of uniform cubic structures.

The understanding of nanocrystal growth by oriented attachment is significantly broadened in the present work. We demonstrate that oriented attachment can take place among α-Fe_2O_3 nanocrystals with a size of more than 100 nm, which is significantly larger than previously observed possible size of primary building blocks (normally less than 10 nm). More importantly, we show that 2D assemblies can also be formed from building blocks by oriented attachment, which previously only exist in nature.[1] These 2D structures can further be assembled into 3D superstructures though dipole–dipole interactions. Based on shape selectivity, 1D nanorods can be assembled into 3D quasi nanocubes by oriented attachment. By constructing these hematite superstructures from unique subunits, the present work significantly expands the applicability of oriented attachment in "bottom-up" construction of nanostructures for their possible applications in electronics, optics or magnetism. The investigation of possible applications of these high-dimensional α-Fe_2O_3 nanostructures in lithium-ion batteries and magnetism is currently undergoing.

Experimental Section

The nanostructures assembled from large α-Fe_2O_3 nanocrystals are obtained through a hydrothermal process. Typically, an aqueous solution of $FeCl_3$ (23.7 mM) contained in a tightly sealed blue-cap glass bottle is aged at 105 °C in an electric oven for 12–50 h. Afterwards, the red product is harvested and washed thoroughly with ultrapure water, before drying at 60 °C overnight. The synthesis of quasi α-Fe_2O_3 nanocubes is based on a similar method, where a 50 mM $FeCl_3$ solution is sealed in a 60 mL Teflon-lined stainless steel autoclave and kept at 160 °C for 1–12 h.

The morphology of products was examined by a transmission electron microscope (TEM; JEOL, JEM-2100F, 200 kV, with electron diffraction) and a field-emission scanning electron miscroscope (FESEM; JEOL, JSM-6700F, 5 kV). Crystallographic information of the samples was investigated with X-ray powder diffraction (XRD; Bruker, D8–Advance X-Ray Diffractometer, $Cu_{K\alpha}$, $\lambda = 1.5406$ Å).

Received: August 27, 2010
Published online: November 9, 2010

Keywords: hematite · nanocubes · oriented attachment · superstructures

[1] J. F. Banfield, S. A. Welch, H. Z. Zhang, T. T. Ebert, R. L. Penn, *Science* **2000**, *289*, 751.
[2] R. L. Penn, J. F. Banfield, *Science* **1998**, *281*, 969.
[3] X. W. Lou, L. A. Archer, Z. C. Yang, *Adv. Mater.* **2008**, *20*, 3987.
[4] X. W. Lou, Y. Wang, C. Yuan, J. Y. Lee, L. A. Archer, *Adv. Mater.* **2006**, *18*, 2325.
[5] H. C. Zeng, *Curr. Nanosci.* **2007**, *3*, 177.
[6] J. S. Chen, C. M. Li, W. W. Zhou, Q. Y. Yan, L. A. Archer, X. W. Lou, *Nanoscale* **2009**, *1*, 280.
[7] J. Li, H. C. Zeng, *J. Am. Chem. Soc.* **2007**, *129*, 15839.
[8] J. Li, H. C. Zeng, *Angew. Chem.* **2005**, *117*, 4416; *Angew. Chem. Int. Ed.* **2005**, *44*, 4342.
[9] J. Zhang, F. Huang, Z. Lin, *Nanoscale* **2010**, *2*, 18.
[10] R. L. Penn, *J. Phys. Chem. B* **2004**, *108*, 12707.
[11] W. K. Koh, A. C. Bartnik, F. W. Wise, C. B. Murray, *J. Am. Chem. Soc.* **2010**, *132*, 3909.
[12] C. Pacholski, A. Kornowski, H. Weller, *Angew. Chem.* **2002**, *114*, 1234; *Angew. Chem. Int. Ed.* **2002**, *41*, 1188.
[13] F. Huang, H. Z. Zhang, J. F. Banfield, *Nano Lett.* **2003**, *3*, 373.
[14] J. H. Yu, J. Joo, H. M. Park, S. I. Baik, Y. W. Kim, S. C. Kim, T. Hyeon, *J. Am. Chem. Soc.* **2005**, *127*, 5662.
[15] F. Huang, H. Z. Zhang, J. F. Banfield, *J. Phys. Chem. B* **2003**, *107*, 10470.
[16] Y. W. Jun, M. F. Casula, J. H. Sim, S. Y. Kim, J. Cheon, A. P. Alivisatos, *J. Am. Chem. Soc.* **2003**, *125*, 15981.
[17] R. L. Penn, J. F. Banfield, *Am. Mineral.* **1998**, *83*, 1077.
[18] C. Ribeiro, C. Vila, J. M. E. de Matos, J. Bettini, E. Longo, E. R. Leite, *Chem. Eur. J.* **2007**, *13*, 5798.
[19] T. Tsuruoka, S. Furukawa, Y. Takashima, K. Yoshida, S. Isoda, S. Kitagawa, *Angew. Chem.* **2009**, *121*, 4833; *Angew. Chem. Int. Ed.* **2009**, *48*, 4739.
[20] R. L. Penn, K. Tanaka, J. Erbs, *J. Cryst. Growth* **2007**, *309*, 97.
[21] R. L. Penn, G. Oskam, T. J. Strathmann, P. C. Searson, A. T. Stone, D. R. Veblen, *J. Phys. Chem. B* **2001**, *105*, 2177.
[22] C. Frandsen, C. R. H. Bahl, B. Lebech, K. Lefmann, L. T. Kuhn, L. Keller, N. H. Andersen, M. von Zimmermann, E. Johnson, S. N. Klausen, S. Mørup, *Phys. Rev. B* **2005**, *72*, 214406.
[23] Y. F. Zhu, W. R. Zhao, H. R. Chen, J. L. Shi, *J. Phys. Chem. C* **2007**, *111*, 5281.
[24] J. S. Chen, Y. L. Tan, C. M. Li, Y. L. Cheah, D. Y. Luan, S. Madhavi, F. Y. C. Boey, L. A. Archer, X. W. Lou, *J. Am. Chem. Soc.* **2010**, *132*, 6124.
[25] K. X. Yao, X. M. Yin, T. H. Wang, H. C. Zeng, *J. Am. Chem. Soc.* **2010**, *132*, 6131.
[26] D. V. Talapin, J. S. Lee, M. V. Kovalenko, E. V. Shevchenko, *Chem. Rev.* **2010**, *110*, 389.
[27] J. S. Chen, T. Zhu, X. H. Yang, H. G. Yang, X. W. Lou, *J. Am. Chem. Soc.* **2010**, 132, 131162.
[28] C. J. Jia, L. D. Sun, F. Luo, X. D. Han, L. J. Heyderman, Z. G. Yan, C. H. Yan, K. Zheng, Z. Zhang, M. Takano, N. Hayashi, M. Eltschka, M. Klaui, U. Rudiger, T. Kasama, L. Cervera-Gontard, R. E. Dunin-Borkowski, G. Tzvetkov, J. Raabe, *J. Am. Chem. Soc.* **2008**, *130*, 16968.
[29] D. V. Talapin, E. V. Shevchenko, C. B. Murray, A. V. Titov, P. Kral, *Nano Lett.* **2007**, *7*, 1213.
[30] M. F. Hansen, C. B. Koch, S. Mørup, *Phys. Rev. B* **2000**, *62*, 1124.
[31] S. Mørup, M. Bo Madsen, J. Franck, J. Villadsen, C. J. W. Koch, *J. Magn. Magn. Mater.* **1983**, *40*, 163.
[32] C. J. Jia, L. D. Sun, Z. G. Yan, L. P. You, F. Luo, X. D. Han, Y. C. Pang, Z. Zhang, C. H. Yan, *Angew. Chem.* **2005**, *117*, 4402; *Angew. Chem. Int. Ed.* **2005**, *44*, 4328.
[33] Y. Piao, J. Kim, H. Bin Na, D. Kim, J. S. Baek, M. K. Ko, J. H. Lee, M. Shokouhimehr, T. Hyeon, *Nat. Mater.* **2008**, *7*, 242.

